Shape-based 3D Level Set Segmentation of the Proximal Femur in CT-Data

Agnes Grünerbl[1], Karl Fritscher[1],
Michael Blauth[2], Volker Kuhn[2] and Rainer Schubert[1]

[1]Institute for Biomedical Image Analysis,
University for Health Science, Medical Informatics and Technology, Tyrol, Austria
[2]Department of Traumatology, University Hospital, Innsbruck, Tyrol, Austria
Email: agnes.gruenerbl@umit.at

Abstract. This work presents the creation of a common shape model of the proximal femur and the use of this common shape model for the automatic segmentation of healthy femora. The method to build up a common shape model is described and the approach of automatic segmentation of CT datasets will be explained. Further the resulting shape model and the use of the model in the segmentation pipeline in order to automatically segment 15 datasets is discussed.

1 Introduction

The presented work is part of a broader project to develop and investigate methods for automated segmentation of the healthy femur in CT-data as well as in x-ray images as a prerequisite for automated positioning of regions of interest for detailed bone analysis.

Even though there has been done some work on segmenting the pelvis and the femur for surgical planning and simulation [e.g. 1, 2, 3], there is few work to find about statistical modelling of the proximal femur and the further use of such a model within a level set based segmentation pipeline.

Therefore, as a first step we aimed to build up a statistical three-dimensional shape model of the proximal femur to serve for automated segmentation of 3D CT-data. This paper will describe the generated shape model and present first results in using this model for automated level set based segmentation of CT-data.

2 State of review

For the creation of 3D statistical shape models different approaches have been introduced: In [4] Rueckert et al. describe the usage of deformation fields to represent shape. Moreover, a number of other approaches to incorporate prior shape knowledge into the segmentation process have been developed [5-10]. Geometric deformable models, also known as geodesic snakes or level set snakes have been developed by Osher and Sethian [11] and have been introduced in the field of image analysis by Caselles and Malladi [13,12]. In [10] Leventon extended

Fig. 1. Left shape model (dark) and shape variation with -1.5 Std. in 1. principal component (light). Middle: shape model. Right: shape model (dark) and shape variation with 1.5 Std. in 1. principal component (light)

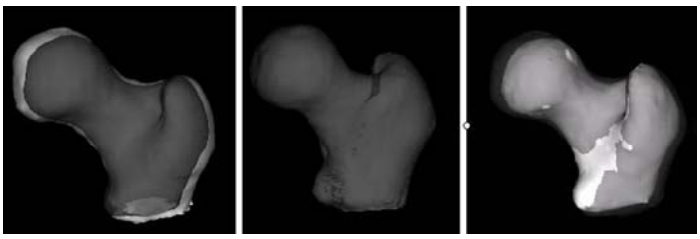

Caselles's geodesic active contours by incorporating prior shape information into the segmentation process. The segmenting-surface evolves according to the image gradient and a maximum a-posteriori (MAP) estimate of the shape and pose parameters of the statistical shape model generated by using principal component analysis.

3 Contributions/Benefits

Using an automatic hierarchic registration approach to initialize the segmentation process and the shape model to guide the segmentation process with level sets gives us the possibility to fully automatically segment the proximal part of the femur in CT-scans.

An important contribution is the possibility to automate the process of segmentation and to make the results reproducible. The automatic approach guarantees that all images are segmented the same way with reproducible results. This means an improvement in the segmentation process and the segmentation quality, since reproduction is not possible in the manual and semi automatic approach because the result here always is influenced by the segmenting expert.

A further benefit of the automatic segmentation approach is, that it is far less time consuming than the semi-automatic approaches such as region growing in combination with essential manual correction.

4 Methods

The first aim of this work was the creation of a common shape model of the proximal femur. In order to create such a shape model, 13 data sets had to be segmented semi-automatically or manually. Out of these segmented images a common shape model could be calculated:

1. rigid alignment of the distance maps of the segmented images onto an atlas image
2. non-rigid alignment of distance maps of labels to atlas label image using demons algorithm [14]
3. Perform PCA on deformation fields, calculated in step 2

Fig. 2. Left: an example for a CT dataset of a proximal Femur with poor quality (slice thickness: 5mm). Right: The result of the automated segmentation of this dataset.

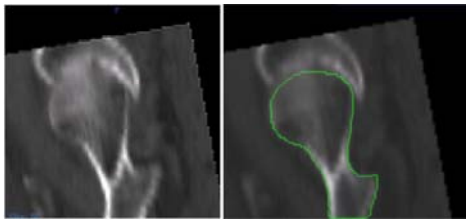

Different instances of shape can be generated by applying the deformation fields resulting from the PCA calculation on the atlas label. Using this shape model in combination with level set segmentation, CT images of the proximal femur were automatically segmented. As an instrument of segmentation the updated and improved version of the segmentation pipeline which was introduced in [15, 16] in order to automatically segment MRI images of the endocardium could be used here. The procedure is as follows:

1. Rigid alignment of the individual image to an atlas image
2. Non rigid alignment of the image to be segmented and the atlas image using demons algorithm
3. Warping atlas label set with deformation field from non rigid registration
4. Rigid alignment of warped label and atlas label to get initial shape parameters
5. Perform PCA decomposition of the resulting deformation field (point 3) to get initial shape parameters
6. Level set segmentation using MAP approach and statistical shape model

Using a shape model relying on 13 manually or semi-automatically segmented datasets, 15 datasets were automatically segmented. Out of these 15 datasets five already had been used to build the shape model. Further the 15 datasets were of different slice-thickness (between 0.625 mm and 5 mm).

In order to evaluate the results of the segmentation, the Similarity Index and the Mean Distance of the resulting segmentation images of the automatic segmentation and the manually slightly corrected final results were calculated.

5 Results

Using the approach described in the method section, a valid common shape model could be created (Fig 1). The first principal component specifies the variation in size. The second and the third principal components specify the variation in the trochanter major and the trochanter minor. The other main components indicate other small variations. Within the first six principal components of the PCA 92% of the shape variations are covered.

The described approach of automatic segmentation has been successfully applied and provided good results for all cases (see Table 1). The evaluation of the segmentation, compared the automatically segmented result and the final,

Table 1. detailed list of the segmentation results with Similarity Index and Mean Distance for all segmented datasets

datasetNo	included /new	Sl-Thickness (mm)	SI	MD
17	new	5	0.903	1.04
22	new	0.625	0.879	1.61
23	new	2.5	0.872	1.64
25	new	1.25	0.875	1.71
27	new	1.25	0.967	0.38
29	new	5	0.975	0.35
30	new	2.5	0.958	0.41
31	included	2.5	0.931	0.59
32	included	2.5	0.915	0.98
34	included	1.25	0.931	0.79
35	new	1.25	0.896	1.5
41	included	1.25	0.911	0.81
42	included	1.25	0.912	1.34
43	new	2.5	0.964	0.52
48	new	2.5	0.962	0.45

manually corrected result, showed that the similarity index averages at 0.9251 with a sigma of 0.043 for the ten totally new datasets.

For the five datasets (31, 31, 34, 41, 42) which were already included into the used shape model the average result of the similarity index was 0.92 with a sigma of 0.01. For the datasets not included the mean distance averages at 0.961 voxel (sigma = 0.59) while the average for the five already included old datasets is 0.902 voxel (sigma = 0.28). This means only a slight difference between the already included and the new datasets. The detailed results can be viewed in Table 1. An interesting result of the automatic segmentation is that the automatic approach produces satisfying results for datasets with all different slice-thicknesses and the segmentation of datasets of high quality does not show better results compared to datasets with poor quality. The left part of Fig. 2 shows such a CT image of poor quality. On the right side of Fig. 2 the result of the automatic segmentation of this image can be seen.

6 Discussion

This preliminary study has shown that the femora can be automatically segmented using the segmentation pipeline developed at IBIA. After the successful creation of a valid common-shape-model this model could effectively be implemented in the segmentation pipeline as initial shape for the level set segmentation. The results of the segmentation of new datasets showed satisfying results using the pipeline and the integrated common shape model.

The main advantage of automatic segmentation can be seen in the time used to segment a dataset. Due to the possibility of automating the segmentation process, in contrast to semi-automatic approaches as region growing, only little interaction of the user is needed. A fast semi-automatic segmentation approach using thresholds is not useful in this case because of the unclear range of grey values for the bones in CT images.

Nevertheless, the results of the evaluation show that further improvement is needed to enhance the accuracy and especially the speed of the segmentation method. In a first step, we expect that the integration of more segmented datasets into the model will further improve the specificity and generality of the model and the quality of the automatic segmentation. Furthermore, the use of grey-value images for a faster segmentation of the Femora in CT images is planed.

References

1. Färber M, Ehrhardt J, Handels H. Automatic atlas-based contour extraction of anatomical structures in medical images. In: Lemke U, et al, editors. CARS. International Congress Series 1281. Elsevier; 2005. p. 272–277.
2. Lamecker H, Seebaß M, Hege HC, Deuflhard P. A 3d statistical shape model of the pelvic bone for segmentation. In: SPIE Medical Imaging. vol. 5370; 2004. p. 1342–1351.
3. Lange T, Tunn PU, Lamecker H, Scheinemann P, Eulenstein S, Schlag P. Computerunterstützte Prothesenkonstruktion mittels statistischen Formmodells bei Beckenresektionen. In: Procs BVM; 2004. p. 30–34.
4. Rueckert D, Frangi A, Schnabel JA. Automatic Construction of 3-D Statistical Deformation Models of the Brain Using Nonrigid Registration. IEEE Trans Med Imaging 2001;22:1014–1025.
5. Cootes TF, Edwards GJ, Taylor C. Active Appearance Models. IEEE Trans Patt Anal Mach Intell 2001;6:681–685.
6. Cootes TF, Taylor CJ, Cooper DH, Graham J. Segmentation and measurement of the cortex from 3-D MR images using coupled surfaces propagation. Comput Vis Image Underst 1995;61:38–59.
7. Zeng X, Staib LH, Schultz R, Duncan JS. Segmentation and measurement of the cortex from 3-D MR images using coupled surfaces propagation. IEEE Trans Med Imaging 1999;18:927–937.
8. Cremers D, Schnorr C, Weickert J. Diffusion-Snakes: Combining Statistical Shape Knowledge and Image Information in a Variational Framework. In: IEEE Workshop on Variational Level Set Methods; 2001. p. 137–144.
9. Paragios N. Priors for level set representations. European Conference on Computer Vision; 2002.
10. Leventon M, Grimson E, Faugeras O. Statistical Shape Influence in Geodesic Active Contours. Comp Vis Patt Rec 2000;1:316–323.
11. Osher J, Sethian JA. Fronts propagating with curvature-dependent speed: algorithms based on Hamilton-Jacobi formulations. J Comp Phys 1988;79:12–49.
12. Malladi R, Sethian J, Vemuri BC. Shape modeling with front propagation: a level set approach. IEEE Trans Patt Anal Mach Intell 1995;17:158–175.
13. Caselles V, Kimmel R, Sapiro G. A geometric model for active contours. Numerische Mathematik 1999;66.
14. Thirion JP. matching as a diffusion process: an analogy with Maxwell's demons. Med Image Anal 1998;2:243–260.
15. Fritscher KD, Pilgram R, Schubert R. Automatic 4D endocardium segmentation using hierarchical registration and model guided level set segmentation. In: Lemke U, et al, editors. CARS. International Congress Series 1281. Elsevier; 2005.
16. Fritscher KD, Schubert R. A software framework for pre-processing and level set segmentation of medical image data. In: SPIE Medical Imaging; 2005.